VII. NUCLEAR MAGNETIC RESONANCE AND HYPERFINE STRUCTURE

Prof. F. Bitter
Prof. L. C. Bradley III
Prof. J. S. Waugh
Dr. P. C. Brot
Dr. H. H. Stroke
Dr. J. F. Waymouth
R. L. Fork
J. V. Gaven, Jr.
H. R. Hirsch
R. J. Hull
C. S. Johnson, Jr.
Ilana Levitan
J. H. Loehlin
F. Mannis
I. G. McWilliams
P. G. Mennitt
S. R. Miller
C. J. Schuler, Jr.
W. W. Smith
C. V. Stager
W. T. Walter

A. LEVEL-CROSSING EXPERIMENT ON Hg^{197*}

A level-crossing experiment was performed in the $6\,^3P_1$ level of Hg^{197*}, the 24-hour isomer of Hg^{197}. The technique used was essentially the same as that employed by Hirsch and Stager (1) to study the Hg^{197} level crossing. However, optical improvements increased the signal-to-noise ratio of the apparatus by a factor of at least 10.

A dip in scattered 2537 A light intensity was observed at a splitting field of 7839.1 ± 1.2 gauss, as measured with a proton-resonance magnetometer probe at a distance approximately 2 cm from the absorption cell. The correction for the cell-to-probe separation, which will probably be several gauss, is still undetermined. The limits of error are simply three times the standard deviation of the magnetometer readings. The cell was illuminated by σ light from the scanning source in order to study $\Delta m = 2$ crossings. The scanning field was 1660 gauss on the Hg^{198} lamp, with the quarter-wave plate and polarizer set to transmit the higher-frequency Zeeman component.

Magnetic scanning curves revealed that, in addition to Hg^{197*}, the cell contained Hg^{196}, Hg^{197}, Hg^{198}, and some natural mercury contamination. The natural mercury contamination was approximately one-third of the total mercury in the cell. Calculations show that none of the other isotopes could have produced the observed intensity dip, and so it must be attributed to Hg^{197*}.

With the use of spectroscopic data (2), calculations show that the Hg^{197*} $F = 15/2$, $m_F = 15/2$ and $F = 13/2$, $m_F = 11/2$ levels should cross at 7870 gauss, which is in remarkable agreement with the experimental results. There are a number of other level crossings in Hg^{197*}. However, consideration of their field strengths, intensities, and linewidths makes our identification certain.

H. R. Hirsch

References

1. H. R. Hirsch and C. V. Stager, Hyperfine structure of Hg^{197}: An application of the level-crossing technique (to be published in J. Opt. Soc. Am.); Quarterly Progress Report No. 57, Research Laboratory of Electronics, M. I. T., April 15, 1960, pp. 57-60.

2. A. C. Melissinos and S. P. Davis, Dipole and quadrupole moments of the isomeric Hg^{197*} nucleus; Isomeric isotope shift, Phys. Rev. 115, 130-137 (1959).

B. FILLING MERCURY-VAPOR LAMPS WITH A KNOWN SMALL NUMBER OF ATOMS

In studying the hyperfine structure of the various isotopes of mercury, it has frequently been necessary to employ electrodeless discharge lamps with a very small number of atoms of the desired isotope, of the order of 10^{12} or 10^{13}. A severe problem in these cases is the phenomenon of "clean-up." After a brief period of operation of the lamp, the desired spectrum disappears; the mercury has cleaned up and is no longer ionized and excited. The factors that influence the rate of this clean-up are not fully understood; in fact, the mechanism is not at all clear. In order to study it more in detail, we decided to run a number of experiments on lamps filled with natural mercury, in the hope, first, of being able to devise specific procedures to avoid the clean-up, and second, to learn more about the mechanisms involved.

A necessary first step in this program was to be able to fill lamps with a known small number of atoms of natural mercury. The number of atoms desired was roughly equivalent, in a 1-cc volume, to the density of saturated mercury vapor at room temperature. The procedure that we adopted, therefore, was to fill the lamp, which had previously been baked out to drive all the mercury out of it, by allowing it to come to equilibrium with a reservoir of natural mercury at 22°C. If the lamp is at a slightly higher temperature than the reservoir, then all the mercury in the lamp should be in the vapor state, and the number of mercury atoms in it could be calculated from the volume and the vapor density. Here, a problem arises. Does a monatomic layer of mercury on quartz have a substantially lower vapor pressure than liquid mercury? It is well known, for instance, that monatomic layers such as cesium or thorium on tungsten show remarkably lower evaporation rates than pure cesium or thorium (1, 2). This question is of considerable importance here because a monatomic layer of mercury on the walls of a cubic cell of 1-cc volume would contain roughly 10 times as many atoms as the vapor at the equilibrium pressure at 22°C; that is, 1μ. Therefore, if such a monolayer could exist, in order to obtain an equilibrium with all the mercury in the cell in the vapor state, the walls would have to be at a temperature high enough so that the vapor pressure of the monolayer would be greater than the 1-μ equilibrium pressure. This temperature could be substantially higher than 22°C.

In order to check this point, the experiment shown schematically in Fig. VII-1 was performed. The cell, C, was connected to the reservoir, R, through a series of constrictions and break-off seals. The cell was in an oven, so that the cell temperature could be varied between room temperature and 700°C. The glassware between the cell and the reservoir was maintained at temperatures around 250°C by another oven. The vapor density in the cell was measured by the scattering of resonance radiation, 2537 A. At the vapor pressures used, the dimensions of the cell were small in comparison with

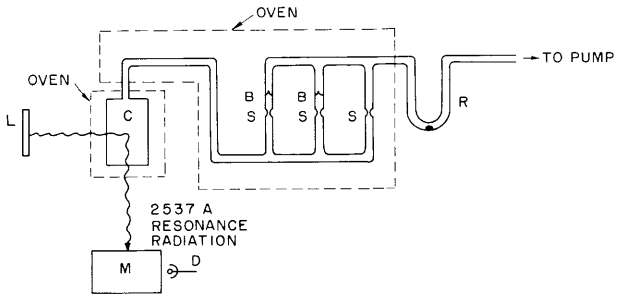

Fig. VII-1. Cell C is connected to mercury reservoir R through break-off seals B and constrictions S. The 2537 A mercury resonance radiation from lamp L is scattered by mercury vapor in the cell and detected by detector D, which is preceded by monochromator M. Under our experimental conditions, when the signal from D is corrected for instrumental background, it is proportional to the density of mercury atoms in the cell, C.

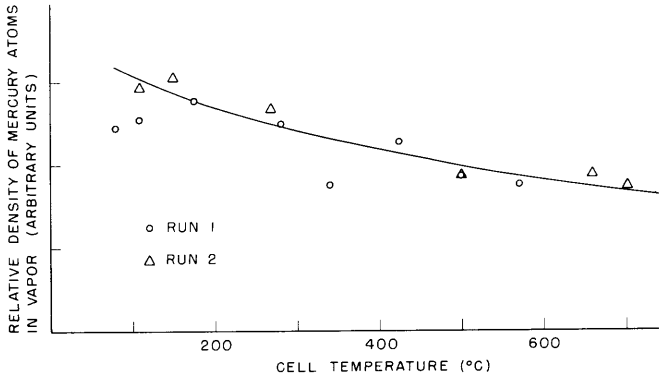

Fig. VII-2. Number of mercury atoms in cell C as a function of temperature. Circles and triangles show the experimental data from two runs; the solid line represents the theoretical prediction of Eq. 2. The deviations of the points below 100°C may possibly indicate monolayer formation.

the photon mean-free path, so that the intensity of resonance radiation scattered into the monochromator, M, was proportional to the density of mercury atoms in the vapor. This proportionality was checked experimentally and was found to hold.

The experiment was performed by allowing the cell, at a temperature of 700°C, to come to equilibrium with the reservoir, which was kept at 22°C. The cell was then sealed off at the constriction S, the power input to the cell oven was turned off, and the cell allowed to cool down. During the cooling-down period, the density of mercury atoms in the cell was monitored continously.

It seems reasonable to suppose that the vapor pressure at 700°C of any hypothetical monolayer will be far in excess of 1μ. If no monolayer forms at any lower temperature,

and the cell could be sealed off without any external appendages, the vapor density in the cell should remain independent of temperature as the cell cools down, until the temperature drops below 22°C. Below this point, its variation with temperature would be determined by the equilibrium vapor pressure of mercury. If a monolayer forms at some higher temperature, the vapor density will decrease at a temperature well above 22°C.

Because we wanted to repeat the experiment several times without opening the system to air, the arrangement of break-off seals was used. This meant that there was additional glassware connected to the cell during the cooling-down period. This "stem" was maintained at a temperature of 250°C. If we assume that the number of mercury atoms in the cell is N_c, and in the stem it is N_s, and that during the cooling-down period no mercury condenses out in a monolayer, then $N_c + N_s = N$ is constant, and

$$\frac{N_c}{V_c}(T_c)^{1/2} = \frac{N_s}{V_s}(T_s)^{1/2} \tag{1}$$

where V_c and V_s are the volumes of the cell and stem, and T_c and T_s are their temperatures.

It is easy to show that if we assume no monolayer formation, the density of atoms in the vapor in the cell, N_c, varies with cell temperature as

$$N_c = \frac{N}{V_s V_c (T_c/T_s)^{1/2} + 1} \tag{2}$$

Figure VII-2 shows a plot of the data obtained from two experimental runs, compared with the prediction of Eq. 2. Clearly, the data are well represented by Eq. 2, except possibly at temperatures below 100°C. Thus, at the present time, the data leave open the question of formation of monolayers at temperatures below 100°C, but provide a recipe for filling cells with a known number of atoms. In order to be certain that the number of atoms in the cell is the equilibrium density multiplied by the volume, that is, that all the mercury in the cell is in the vapor state, it is necessary to maintain the cell at a temperature higher than 100°C up to the instant of sealing off. We expect to obtain more data on the behavior of the sealed-off cells at temperatures below 100°C.

J. F. Waymouth, S. W. Thompson,
L. C. Bradley III, H. H. Stroke

References

1. J. A. Becker, Phys. Rev. 28, 341 (1926).
2. I. Langmuir, Phys. Rev. 43, 224 (1933).

C. INTENSITIES IN LEVEL-CROSSING EXPERIMENTS

In a level-crossing experiment (1) a change in intensity of scattered light is observed at the magnetic field that causes two Zeeman levels of the scattering atom to become degenerate. The magnitude of this change can be calculated from two formulas given by Colgrove, Franken, Lewis, and Sands (2):

$$R_s = k\left[\left|(A|\vec{e}_2\cdot\vec{r}|B)(B|\vec{e}_1\cdot\vec{r}|A)\right|^2+\left|(A|\vec{e}_2\cdot\vec{r}|C)(C|\vec{e}_1\cdot\vec{r}|A)\right|^2\right] \tag{1}$$

$$R_+ = k\left[\left|(A|\vec{e}_2\cdot\vec{r}|B)(B|\vec{e}_1\cdot\vec{r}|A)+(A|\vec{e}_2\cdot\vec{r}|C)(C|\vec{e}_1\cdot\vec{r}|A)\right|^2\right] \tag{2}$$

where k is a constant, and r is the coordinate of the electron that is excited.

Either R_s or R_+ gives the rate at which photons with polarization vector $\vec{e}_1$ transfer atoms from state $|A)$ to states $|B)$ or $|C)$, reradiate with polarization vector $\vec{e}_2$, and return the atoms to state $|A)$: R_s is used if the energies of $|B)$ and $|C)$ differ by well over a natural linewidth; R_+ applies if $|B)$ and $|C)$ are degenerate. The level-crossing peak, or dip, is simply $R_+ - R_s$. The use of $|B)$ and $|C)$ in Eqs. 1 and 2 implies that the state vectors do not differ in the degenerate and nondegenerate cases. This is not necessarily so. A theorem of matrix algebra states that it is possible to find a pair of unit orthogonal eigenvectors for every doubly degenerate eigenvalue of a matrix, but that the pair is not uniquely determined. The most general orthonormal eigenvectors in the doubly degenerate case are

$$|X) = \frac{1}{(1+p^2)^{1/2}}\left[|B)+p|C)\right]$$

$$|Y) = \frac{|p|}{(1+p^2)^{1/2}}\left[|B)-\frac{1}{p^*}|C)\right]$$

where p is a complex constant. Then the most general expression for the transition rate at the level crossing is

$$R'_+ = k\left[\left|(A|\vec{e}_2\cdot\vec{r}|X)(X|\vec{e}_1\cdot\vec{r}|A)+(A|\vec{e}_2\cdot\vec{r}|Y)(Y|\vec{e}_1\cdot\vec{r}|A)\right|^2\right] \tag{3}$$

A few algebraic steps show that $R'_+ = R_+$, and, therefore, that it is proper to use the specialized wave functions, $|B)$ and $|C)$ as in Eq. 2.

Equation 2 has been used to compute the depth of the level-crossing dip that was expected in an experiment recently performed on Hg^{199} by Hirsch (3). First, it is necessary to expand the intermediate field wave functions $|B)$ and $|C)$ in terms of zero-field wave functions. This is done by the usual procedure of substituting the energy at the level crossing in the Hamiltonian matrix. Then, at or near the crossing field,

$$|B) = |3/2, -3/2)$$

$$|C) = -\frac{1}{3}|3/2, 1/2) + \frac{2\sqrt{2}}{3}|1/2, 1/2)$$

where the zero-field wave functions are in the form $|F, m_F)$.

The vector $\vec{e}_1$ is taken on the x-axis, and $\vec{e}_2$ on the y-axis. Condon and Shortley (4) give the matrix elements of $\vec{r}$ in formulas $9^3(11)$ and $11^3(8)$. All of the elements are preceded by the same reduced matrix element, which cancels out in the ratio

$$\alpha = \frac{R_+ - R_s}{R_s} = 0.9973$$

Here, α is the fractional change in intensity at the level crossing. In other words, 99 73/100 per cent of the scanning peak should vanish at the level crossing if the following conditions hold:

(a) The magnet is perfectly homogeneous.

(b) The solid angle subtended by the detector is small.

(c) The illumination is a parallel beam of pure σ light.

(d) Changes in penetration depth are negligible.

The experimental value of α, α_x, is 0.17, and thus it is evident that some of these conditions have not been met.

When parts of the cell are masked, the linewidth decreases as much as 40 per cent, which indicates magnet inhomogeneity. If the depth of the cell were reduced, it is likely that the linewidth would be still less. The linewidth calculated from the lifetime of the $^3P_1$ level (4) is 0.93 gauss, and measured linewidths are approximately 3 gauss with the present apparatus. Thus, condition (a) appears to be critical.

Condition (b) is well satisfied. When the solid angle subtended by the detector is increased by a factor of more than 5, there is little change in α_x. Rough estimates indicate that changes in penetration depth and imperfect illumination are less responsible for the low value of α_x than the effect of magnet inhomogeneity.

It appears that limitations of the apparatus make it difficult to achieve the theoretical intensity change.

H. R. Hirsch

References

1. H. R. Hirsch and C. V. Stager, Hyperfine structure of Hg^{197}: An application of the level-crossing technique (to be published in J. Opt. Soc. Am.); Quarterly Progress Report, No. 57, Research Laboratory of Electronics, M. I. T., April 15, 1960, pp. 57-60.

2. F. D. Colgrove, P. A. Franken, R. R. Lewis, and R. H. Sands, Novel methods of spectroscopy with applications to precision fine structure measurements, Phys. Rev. Letters 3, 420 (1959).

3. H. R. Hirsch, Bull. Am. Phys. Soc. Ser. II, Vol. 5, p. 274, 1960 (Abstract).

4. E. U. Condon and G. H. Shortley, The Theory of Atomic Spectra (Cambridge University Press, London, 1957).

D. CONFIGURATION MIXING AND THE EFFECTS OF DISTRIBUTED NUCLEAR MAGNETIZATION ON HYPERFINE STRUCTURE IN ODD A NUCLEI

A property of the nucleus that is closely related to the magnetic moment is the spatial distribution of its magnetization. This is manifested by the magnetic interaction of the nucleus with penetrating electrons. Bohr and Weisskopf (BW) developed the theory for the hyperfine-structure interaction ("BW Effect"), using a single-particle model for the magnetic moment and a uniform nuclear charge distribution (1). Bohr (2) and Reiner (3) have treated the problem within the framework of the collective or asymmetric model. Our experiments on the hfs of several cesium isotopes (4) had indicated that agreement with experiment would be possible only if some details about the nucleon configurations were included in the BW theory. We therefore developed a formalism that considers configuration-mixing effects as used by Blin-Stoyle (5), Arima and Horie (6), and Noya, Arima, and Horie (7) for magnetic moments. We find that the BW effect may be used in conjunction with magnetic-moment data to determine admixtures of excited configurations.

Consider atoms with angular momentum $J = 1/2$. The hfs separation between the levels $F = I \pm 1/2$ is $\Delta\nu$, where I is the nuclear spin. The hfs energy of the state $F = I + 1/2$ is $W = Ih\Delta\nu/(2I+1)$. From BW we obtain

$$W_S = \pm \frac{16\pi e}{3} \int_N \sum_i d\tau_N \psi_N^* \left[g_S^{(i)} \hat{S}_Z^{(i)} \int_{R_i}^{\infty} FG\, dr + g_S^{(i)} \hat{\underline{A}}^{(i)}_Z \int_0^{R_i} \frac{r^3}{R_i^3} FG\, dr \right] \psi_N \tag{1a}$$

with the spin asymmetry operator given by

$$\hat{\underline{A}} = -\sqrt{2\pi}\left[\hat{S} \times \hat{Y}^2(\theta, \phi)\right]^1 \tag{1b}$$

and

$$W_L = \pm \frac{16\pi e}{3} \int_N \sum_i d\tau_N \psi_N^* g_L^{(i)} \hat{L}_Z^{(i)} \left[\int_{R_i}^{\infty} FG\, dr + \int_0^{R_i} \frac{r^3}{R_i^3} FG\, dr \right] \tag{2}$$

The symbols W_S and W_L represent spin and orbital parts of W; N, the nuclear volume; F and G, Dirac electron wave functions for the extended nucleus; ψ_N, nuclear wave function corresponding to the maximum Z component of the spin; i, the i^{th} nucleon; R_i, the nucleon coordinate; r, electron coordinate; $g_S^{(i)}$ and $g_L^{(i)}$, spin and orbital g values of the i^{th} nucleon; and e, electron charge. The plus and minus signs indicate $s_{1/2}$ and $p_{1/2}$ electrons. By writing

$$W_{extended} = W_{point}(1+\epsilon) \tag{3}$$

we find that

$$-\epsilon = \frac{1}{\mu \int_0^\infty F_o G_o \, dr} \left\{ \int_N \sum_i d\tau_N \psi_N^* \left[g_S^{(i)} \left(\hat{S}_Z^{(i)} \int_0^{R_i} FG \, dr - \hat{\underline{A}}_Z^{(i)} \int_0^{R_i} \frac{FGr^3}{R_i^3} \, dr \right) \right.\right.$$

$$\left.\left. + g_L^{(i)} \hat{L}_Z^{(i)} \int_0^{R_i} \left(1 - \frac{r^3}{R_i^3} \right) FG \, dr \right] \psi_N \right\} \tag{4}$$

Here F_o and G_o are the electron wave functions for a point charge, and μ is the nuclear magnetic moment. Our problem is twofold: to obtain the solution for the electron wave function with the actual nuclear charge distribution, and to calculate the required nuclear matrix elements.

We have taken for the charge distribution, ρ, the trapezoidal form of Hahn, Ravenhall, and Hofstader (8). By approximating it with the polynomial

$$\rho = \rho_o + \rho_2 x^2 + \rho_3 x^3 + \rho_4 x^4 \tag{5}$$

where $x = R/R_N$, R is the distance from the center of the nucleus, and R_N, the extent of the charge distribution, we obtain a series solution of the Dirac equation for the electron in a form similar to BW. The terms $n = 1, 2$ yield an accuracy of a few per cent; Eq. 4 then becomes

$$-\epsilon = \frac{1}{\mu} \left\{ \int_N \sum_i d\tau_N \psi_N^* \frac{R_i^{2n}}{R_N^{2n}} \left[g_S^{(i)} \left(\hat{S}_Z^{(i)} b_{S_{2n}} - \hat{\underline{A}}_Z^{(i)} b_{\underline{A}_{2n}} \right) + g_L^{(i)} \hat{L}_Z^{(i)} b_{L_{2n}} \right] \psi_N \right\} \tag{6}$$

where the b are combinations of the coefficients appearing in the series solution.

The nuclear matrix elements were calculated for the types of admixtures used by Noya, Arima, and Horie (7). We find the contribution of the term for $\Delta \ell = 2$ excitations usually small, so that we can write

$$-\epsilon = \frac{1}{\mu} \left\{ a_{S_{sp}} g_S B_S + a_{L_{sp}} g_L B_L + \sum_i a_o^{(i)} \left[B_S^{(i)} g_S^{(i)} + B_L^{(i)} g_L^{(i)} \right] \right\} \tag{7}$$

where sp denotes the single-particle contribution, and the factors B are functions of b, nuclear radial integrals (calculated for a Saxon-Woods potential well), and the ratio of reduced matrix elements $\langle \| \hat{\underline{A}} \| \rangle / \langle \| \hat{S} \| \rangle$. The $a_o^{(i)}$ depend on the admixtures with $\Delta \ell = 0$. Similarly, we write

$$\mu = a_{S_{sp}} g_S + a_{L_{sp}} g_L + \sum_i a_o^{(i)} \left(g_S^{(i)} - g_L^{(i)} \right) \tag{8}$$

By comparing Eqs. 7 and 8, we see the possibility of obtaining the unknowns, a_o, for two likely admixtures, from the experimental data of μ and ϵ. Comparisons

between theory and experiment made thus far are generally satisfactory.

We are indebted to Dr. L. M. Delves for his assistance, and for the use of his program for calculating radial matrix elements and energies, and to Mr. Peter Hodgson for the programming work on the Mercury computer at Oxford University. We also thank Miss Mida Karakashian, of M. I. T., for her work in programming the electron coefficient problem for the LGP 30 computer.

H. H. Stroke, R. J. Blin-Stoyle

[Professor Blin-Stoyle is a member of the Department of Physics and the Laboratory for Nuclear Science, M. I. T.; on leave from the Clarendon Laboratory, Oxford University.]

References

1. A. Bohr and V. F. Weisskopf, Phys. Rev. 77, 94 (1950).

2. A. Bohr, Phys. Rev. 81, 331 (1951).

3. A. S. Reiner, Nuclear Phys. 5, 544 (1958); Ph. D. Thesis, University of Amsterdam, Netherlands, 1958.

4. H. H. Stroke, V. Jaccarino, D. S. Edmonds, Jr., and R. Weiss, Phys. Rev. 105, 590 (1957).

5. R. J. Blin-Stoyle, Proc. Phys. Soc. (London) A66, 1158 (1953).

6. A. Arima and H. Horie, Progr. Theoret. Phys. (Kyoto) 12, 623 (1954).

7. H. Noya, A. Arima, and H. Horie, Progr. Theoret. Phys. (Kyoto) (Supplement) 8, 33 (1958).

8. B. Hahn, D. G. Ravenhall, and R. Hofstader, Phys. Rev. 101, 1131 (1956).

E. ZEEMAN EFFECT OF THE HYPERFINE STRUCTURE IN AN sp CONFIGURATION

The effect of the nuclear dipole moment, quadrupole moment, and magnetic field on an sp electron configuration has been calculated. General formulas were obtained for the matrix of the Hamiltonian in the IJF representation as functions of I, F, and H (the magnetic field) that permit direct application to any isotope of any atom with an sp configuration.

In the L-S coupling scheme, the sp configuration gives rise to a triplet and a singlet $\left({}^3P_{0,1,2} \text{ and } {}^1P_1\right)$. Breit and Wills (1) have shown that for intermediate coupling these states may be written as linear combinations of j-j coupling wave functions. In our treatment we assume no configuration mixing.

$$\psi\left({}^3P_2\right) = \left(\frac{1}{2}\,\frac{3}{2}\right)_2$$

and

$$\psi\left({}^3P_1\right) = c_1\left(\tfrac{1}{2}\,\tfrac{3}{2}\right)_1 + c_2\left(\tfrac{1}{2}\,\tfrac{1}{2}\right)_1$$

$$\psi\left({}^3P_0\right) = \left(\tfrac{1}{2}\,\tfrac{1}{2}\right)_0$$

$$\psi\left({}^1P_1\right) = c_2\left(\tfrac{1}{2}\,\tfrac{3}{2}\right)_1 - c_1\left(\tfrac{1}{2}\,\tfrac{1}{2}\right)_1$$

where c_1 and c_2 are obtained from the measured g-value (1) of the ${}^3P_1$ state.

Following Schwartz (2), we may write the hfs Hamiltonian $\underline{H}_1 = \sum_{k,\,i} T_i^{(k)} \cdot N^{(k)}$, where $T_i^{(k)}$ is a tensor operator of rank k operating in the space of the i^{th} electron coordinates, and $N^{(k)}$ operates in the space of the nucleon coordinates. The matrix elements of $\underline{H}_1$ have the form $\sum_k \left\langle IJ'F'M'_F \middle| \sum_i T_i^{(k)} \cdot N^{(k)} \middle| IJFM_F \right\rangle$. Using a theorem of Racah (3), we obtain

$$\sum_k \left\langle IJ'F'M_F \middle| \sum_i T_i^{(k)} \cdot N^{(k)} \middle| IJFM_F \right\rangle = \sum_k (-1)^{I+J+F'} \delta_{FF'} \delta_{M_F M'_F}$$

$$\times \begin{Bmatrix} F & J' & I \\ k & I & J \end{Bmatrix} \left\langle I \| N^{(k)} \| I \right\rangle \left\langle J' \| \sum_i T_i^{(k)} \| J \right\rangle$$

The brace is the Wigner 6-J symbol (4), and the double bars indicate reduced matrix elements (4).

The magnetic field Hamiltonian is written as $\underline{H}_2 = (g_L L_z + g_S S_z - g_I I_z)\, H$, where H is the magnetic field assumed to be in the z-direction. Extracting the F and M_F dependence by means of the theorem used above, we obtain

$$\left\langle IJ'F'M_F \middle| \underline{H}_2 \middle| IJFM_F \right\rangle = (-1)^{F'+F-M_F+I+J+1} \begin{pmatrix} F' & 1 & F \\ -M_F & 0 & M_F \end{pmatrix} \left[(2F+1)(2F'+1)\right]^{1/2}$$

$$\times \begin{Bmatrix} J' & F' & I \\ F & J & 1 \end{Bmatrix} \left\langle J' \| \underline{H}_2 \| J \right\rangle H$$

where the expression in large parentheses represents the Wigner 3-J symbol (4). We calculate general formulas in terms of I, F, and J for the matrix elements in the representation, where $\underline{H}_1 = \underline{H}_2 = 0$ and spin-orbit interaction and configuration mixing are neglected. For convenience, M_F is redefined as m.

a. Hyperfine-Structure Matrix Elements

Diagonal dipole elements (k = 1; here, k represents the superscript on $\underline{H}^{(k)}$):

$$\left\langle {}^3P_2 IF \middle| \underline{H}_1^{(1)} \middle| {}^3P_2 IF \right\rangle = \frac{F(F+1) - I(I+1) - 6}{2} \left\{ \frac{a_s}{4} + \frac{3a_{3/2}}{4} \right\}$$

$$\left\langle {}^3P_1 IF \left| \underline{H}_1^{(1)} \right| {}^3P_1 IF \right\rangle = \frac{F(F+1) - I(I+1) - 2}{2} \left\{ \left(\frac{c_2^2}{2} - \frac{c_1^2}{4} \right) a_s + \frac{c_2^2}{2} a_{1/2} + \left(\frac{5}{4} c_1^2 - \frac{5}{16} \sqrt{2} \xi c_1 c_2 \right) a_{3/2} \right\}$$

Off-diagonal dipole elements (k=1):

$$\left\langle {}^3P_2 IF \left| \underline{H}_1^{(1)} \right| {}^3P_1 IF \right\rangle = - \frac{\left[(F+I+3)(I+2-F)(F+2-I)(F+I-1) \right]^{1/2}}{4} \times \left\{ \frac{c_1}{2} a_s - \frac{c_1}{2} + \frac{5\sqrt{2}}{16} c_2 \xi \right\} a_{3/2}$$

$$\left\langle {}^3P_o IF \left| \underline{H}_1^{(1)} \right| {}^3P_1 IF \right\rangle = \frac{1}{\sqrt{8}} \left[(F+I+2)(I+1-F)(F+1-I)(F+I) \right]^{1/2} \times \left\{ \frac{c_2}{\sqrt{2}} a_s - \frac{c_2}{\sqrt{2}} a_{1/2} - \frac{5}{8} \xi c_1 a_{3/2} \right\}$$

$$\left\langle {}^1P_1 IF \left| \underline{H}_1^{(1)} \right| {}^3P_1 IF \right\rangle = - \frac{F(F+1) - I(I+1) - 2}{2} \left\{ \frac{3 c_1 c_2}{4} a_s + \frac{c_1 c_2}{2} a_{1/2} + \left[\frac{5 \left(c_2^2 - c_1^2 \right)}{32} \sqrt{2} \xi - \frac{5}{4} c_1 c_2 \right] a_{3/2} \right\}$$

Diagonal quadrupole elements (k=2):

$$\left\langle {}^3P_2 IF \left| \underline{H}_1^{(2)} \right| {}^3P_2 IF \right\rangle = \frac{\kappa(\kappa+1) - 8I(I+1)}{8(2I-1)(2I)} b_{3/2} \qquad \kappa = F(F+1) - I(I+1) - 6$$

$$\left\langle {}^3P_1 IF \left| \underline{H}_1^{(2)} \right| {}^3P_1 IF \right\rangle = \frac{\kappa'(\kappa'+1) - 8I(I+1)}{4(2I-1)(2I)} \left\{ \frac{c_1^2}{2} + c_1 c_2 \sqrt{2} \eta \right\} b_{3/2} \qquad \kappa' = F(F+1) - I(I+1) - 2$$

Off-diagonal quadrupole elements (k=2):

$$\left\langle {}^3P_2 IF \left| \underline{H}_1^{(2)} \right| {}^3P_1 IF \right\rangle = - \frac{1}{16I(2I-1)} \left[(F+I+3)(F+2-F)(F+2-I)(F+I-1) \right]^{1/2} \times \left[F(F+1) - I(I+1) - 3 \right] \left\{ (c_1 + \sqrt{2} \eta c_2) b_{3/2} \right\}$$

$$\left\langle {}^1P_1 IF \left| \underline{H}_1^{(2)} \right| {}^3P_2 IF \right\rangle = \frac{3(\kappa')(\kappa'+1) - 8I(I+1)}{4(2I-1)(2I)} \left\{ \frac{c_1 c_2}{2} - \frac{\left(c_1^2 - c_2^2 \right)}{2} \sqrt{2} \eta \right\} b_{3/2}$$

In the expressions given above a_s, $a_{1/2}$, $a_{3/2}$ are the dipole hfs interaction constants for the s electron and the p electron in the states s, j = 1/2, and j = 3/2, respectively; $b_{3/2}$ is the quadrupole interaction for a $p_{3/2}$ electron; ξ and η are ratios of certain radial integrals as given by Schwartz (2).

b. Matrix Elements of the Magnetic-Field Interaction

In the following expressions, a superscript zero denotes the unperturbed zero-order wave functions, and nonrelativistic electrons are assumed.

Elements diagonal in J:

$$\left\langle {}^3P^o_{J,F} \left| \underline{H}_2 \right| {}^3P^o_{J,F} \right\rangle = \frac{m\hbar H}{2F(F+1)} \left[g_J[J(J+1)+F(F+1)-I(I+1)] + g_I[I(I+1)+F(F+1)-J(J+1)] \right]$$

$$\left\langle {}^3P^o_{J,F-1} \left| \underline{H}_2 \right| {}^3P^o_{J,F} \right\rangle = \frac{\hbar H(g_I+g_J)}{2F} \left[\frac{(F^2-m^2)[(I+J+1)^2-F^2][F^2-(I-J)^2]}{(4F^2-1)} \right]^{1/2}$$

Elements off-diagonal in J:

$$\left\langle {}^3P^o_{J-1,F} \left| \underline{H}_2 \right| {}^3P^o_{J,F} \right\rangle = \frac{m\hbar H(g_L-g_S)}{4F(F+1)} \left[\frac{[(I+F+1)^2-J^2][J^2-(I-F)^2][9-J^2]}{4J^2-1} \right]^{1/2}$$

$$\left\langle {}^3P^o_{J-1,F-1} \left| \underline{H}_2 \right| {}^3P^o_{J,F} \right\rangle = \frac{-\hbar H(g_L-g_S)}{4F} \left[\frac{(F^2-m^2)[(F+J)^2-J^2][(F+J)^2-(I+1)^2](9-J^2)}{(4F^2-1)(4J^2-1)} \right]^{1/2}$$

The spin-orbit interaction may now be taken into account by writing the wave functions as linear combinations of the L-S coupling wave functions:

$$\psi\left({}^3P_2\right) = \left| {}^3P^o_2 \right\rangle$$

$$\psi\left({}^3P_1\right) = a\left| {}^3P^o_1 \right\rangle + b\left| {}^1P^o_1 \right\rangle$$

$$\psi\left({}^3P_o\right) = \left| {}^3P^o_o \right\rangle$$

$$\psi\left({}^1P_1\right) = -b\left| {}^3P^o_1 \right\rangle + a\left| {}^1P^o_1 \right\rangle$$

The coefficients a and b are related (5) to c_1 and c_2 by

$$c_1 = \sqrt{1/3}a - \sqrt{2/3}b$$

$$c_2 = \sqrt{2/3}a + \sqrt{1/3}b$$

With this expansion of the wave functions, we obtain the desired matrix which is diagonal in the zero-order case, $\underline{H}_1 = \underline{H}_2 = 0$, with the spin-orbit interaction now not equal to zero. The desired matrix elements are now given in terms of a, b and the matrix elements given above. For simplicity, we resort to the following convention. The symbol $\langle {}^{n'}P_{J', F'} | H_2 | {}^{n}P_{J, F} \rangle (g'_x \rightarrow g_x)$ is to be read as $\langle {}^{n'}P_{J', F'} | H_2 | {}^{n}P_{J, F} \rangle$ with g_x replaced by g'_x. The g factors have the meaning; g'_J is the experimental electronic g factor, $g_I = -\mu/I$, where μ is the experimental magnetic moment, and g_L and g_S are the free-electron orbit and spin g values.

The matrix elements for the spin-orbit interaction perturbed states in terms of the unperturbed elements are then:

$$\langle {}^3P_{J, F'} | \underline{H}_2 | {}^3P_{J, F} \rangle = \langle {}^3P^o_{J, F'} | \underline{H}_2 | {}^3P^o_{J, F} \rangle (g_{J'} \rightarrow g_J)$$

$$\langle {}^3P_{J-1, F'} | \underline{H}_2 | {}^3P_{J, F} \rangle = a \langle {}^3P^o_{J-1, F'} | \underline{H}_2 | {}^3P^o_{J, F} \rangle$$

$$\langle {}^1P_{J, F'} | \underline{H}_2 | {}^1P_{J, F} \rangle = \langle {}^3P^o_{J, F'} | \underline{H}_2 | {}^3P^o_{J, F} \rangle (g_L \rightarrow g_J)$$

$$\langle {}^3P_{J, F'} | \underline{H}_2 | {}^1P_{J, F} \rangle = -ab \langle {}^3P^o_{J, F'} | \underline{H}_2 | {}^3P^o_{J, F} \rangle + ab \langle {}^3P^o_{J, F'} | \underline{H}_2 | {}^3P^o_{J, F} \rangle (g_L \rightarrow g_J)$$

$$\langle {}^3P_{J-1, F'} | \underline{H}_2 | {}^1P_{J, F} \rangle = -b \langle {}^3P^o_{J-1, F'} | \underline{H}_2 | {}^3P^o_{J, F} \rangle$$

We now have the complete matrix $\langle {}^{2s'+1}P_{J'} IF'M' | \underline{H}_1 + \underline{H}_2 | {}^{2s+1}P_J IFM \rangle$. In order to find the energies, we first diagonalize the submatrices that are diagonal in the zero-order states; by zero-order states we mean the eigenstates when $\underline{H}_1 = \underline{H}_2 = 0$. The diagonal elements are a close approximation to the actual energy levels, and the transformed off-diagonal elements represent small corrections to these values. Thus it is possible to calculate the energy corrections to a high degree of accuracy by second-order perturbation theory. Exact diagonalization of the matrix by the use of a computer is an alternative approach.

We have succeeded in expressing energy-level separations in terms of the hfs interaction constants for the individual electrons. By taking into account the off-diagonal elements of the hfs interaction and the magnetic field, we can obtain the individual electron-interaction constants with an accuracy comparable to that with which the energy-level separations are measured, provided that configuration interaction may be neglected.

R. L. Fork, C. V. Stager, L. C. Bradley III

References

1. G. Breit and L. Wills, Phys. Rev. 44, 470 (1933).

2. C. Schwartz, Phys. Rev. 97, 380 (1955).

3. G. Racah, Phys. Rev. 62, 438 (1942).

4. A. R. Edmonds, Angular Momentum in Quantum Mechanics (Princeton University Press, Princeton, N. J., 1957), pp. 75, 92, 111.

5. H. Kopfermann, Nuclear Moments (Academic Press, New York, 1958), p. 150.